Demonstration of cluster-state shaping and quantum erasure for continuous variables

Yoshichika Miwa,[1] Ryuji Ukai,[1] Jun-ichi Yoshikawa,[1] Radim Filip,[2] Peter van Loock,[3] and Akira Furusawa[1]

[1]*Department of Applied Physics, School of Engineering, The University of Tokyo, 7-3-1 Hongo, Bunkyo-ku, Tokyo 113-8656, Japan*
[2]*Department of Optics, Palacký University, 17 listopadu 50, 772 07 Olomouc, Czech Republic*
[3]*Optical Quantum Information Theory Group, Max Planck Institute for the Science of Light, Institute of Theoretical Physics I,*
Universität Erlangen-Nürnberg, Staudtstrasse 7/B2, D-91058 Erlangen, Germany

We demonstrate experimentally how to remove an arbitrary node from a continuous-variable cluster state and how to shorten any quantum wires of such a state. These two basic operations, performed in an unconditional fashion, are a manifestation of quantum erasure and can be employed to obtain various graph states from an initial cluster state. Starting with a sufficiently large cluster, the resulting graph states can then be used for universal quantum information processing. In the experiment, all variations of this cluster shaping are demonstrated on a four-mode linear cluster state through homodyne measurements and feedforward.

PACS number(s): 03.67.Lx, 42.50.Dv, 42.50.Ex

I. INTRODUCTION

A one-way quantum computer uses a cluster state as a resource [1,2]. For qubits, cluster states have a graph structure where the nodes are qubits, while the bonds represent controlled π-phase-shift interactions [1]. Instead of the computational basis for a qubit ($|0\rangle$,$|1\rangle$), coordinate eigenstates $|x\rangle$ for any real number x correspond to the computational basis in the continuous-variable (CV) case. A very powerful scheme for generating a large-scale but fixed CV cluster state in just one time step was recently proposed in Ref. [3] using optical frequency combs. Starting with such large-scale cluster states enables one to use a top-to-bottom approach, in which the initial state can be shaped and converted into a modified, smaller cluster state suitable for a given quantum computation task. In order to adapt the fixed initial cluster state to any desired operation, we need to be able to flexibly shape the cluster state.

For CV cluster states, the nodes are quantized optical modes coupled through quantum nondemolition (QND) interactions [2]. Once these cluster nodes are linked, they can be easily decoupled by measurements in the computational basis and feedforward, as we have reported for the CV case [4,5]. This decoupling is a manifestation of a complete CV quantum erasure which works independently of the input states for this QND-type interaction. Only two basic shaping operations are required to shrink a fixed large-scale cluster state and transform it into an appropriate form for a desired quantum operation [6]. One is the removal of unwanted nodes by measuring the modes to be removed and performing feedforward on the neighboring modes, at the same time breaking all bonds between that node and the rest (here feedforward corresponds to phase-space displacements depending on the homodyne measurement results). The other operation is wire shortening [6], which also removes modes from a cluster state but leaves the neighboring modes connected in the resulting graph state.

In this article, we demonstrate unconditional cluster-state shaping for CV cluster states, specifically, for a CV four-mode linear cluster state. Similar to the qubit case, feedforward corrections are essential to accomplish the cluster shaping. However, so far, cluster shaping has not been demonstrated in a deterministic and unconditional fashion since the single-photon-based qubit proposals [7] and implementations [8] are typically heralded, relying on postselection. In contrast, the CV approach for creating and shaping cluster states does not require any quantum memories for storage. The price for this unconditionality, however, is that the finitely squeezed CV cluster states are intrinsically imperfect [2,9,10].

II. THEORY

Each quantum mode can be represented by a pair of observables $\hat{x}$ and $\hat{p}$ in a Heisenberg picture, where these operators are the real and imaginary parts of each mode's annihilation operator, $\hat{a} = \hat{x} + i\hat{p}$. The commutation relation of these operators is $[\hat{x}_i, \hat{p}_j] = i\delta_{ij}/2$ with $\hbar = 1/2$; the subscripts i and j refer to the ith and jth modes, respectively. In quantum optics, these observables represent the electric field amplitudes in two orthogonal quadratures of each spatial mode.

CV cluster states are defined via the following stabilizer combinations [9,11] (so-called nullifiers [6]):

$$\left(\hat{p}_i - \sum_{j \in N_i} \hat{x}_j \right), \quad \forall i \in G. \qquad (1)$$

Here nullifiers mean that the states become zero eigenstates of these quadrature combinations in the limit of infinite squeezing. The modes of $i \in G$ correspond to the nodes of the graph G, while the modes of $j \in N_i$ are the nearest neighbors of the ith mode. The cluster state can be created by preparing $|p = 0\rangle$ for each mode of $i \in G$ and performing QND interactions with modes of $j \in N_i$, where the unitary operator for the QND interaction is $\hat{U}_{ij} = \exp(2i\hat{x}_i\hat{x}_j)$ [12].

With finite squeezing, the quadrature correlations are imperfect. As sufficient conditions for cluster-type entanglement, we can use the following inequalities:

$$\left\langle \Delta \left(\hat{p}_i - \sum_{j \in N_i} \hat{x}_j \right)^2 \right\rangle < \frac{1}{2}, \quad \forall i \in G, \qquad (2)$$

because for any $i \in G$ and $j \in N_i$, we can derive

$$\left\langle \Delta \left(\hat{p}_i - \hat{x}_j - \sum_{k \in N_{i|j}} \hat{x}_k \right)^2 \right\rangle + \left\langle \Delta \left(\hat{p}_j - \hat{x}_i - \sum_{l \in N_{j|i}} \hat{x}_l \right)^2 \right\rangle < 1,$$
(3)

where $N_{i|j}$ denotes the set of all neighbor modes of the ith mode, except for the jth mode. This equation proves that the ith and jth modes are entangled, according to the criteria of Ref. [13].

We can reverse the QND interaction and restore one of two unknown input states by using homodyne measurements and feedforward [4,5]. This restoration also does not depend on the specific interaction strength of the QND interaction. In this case, the inverse QND interaction between the ith and jth modes $\hat{U}_{ij}^\dagger = \exp(-2i\hat{x}_i\hat{x}_j)$ can be decomposed into a homodyne measurement of the x quadrature of the jth mode with a subsequent phase-space displacement $\hat{Z}_i(x_j) = \exp(-2i\hat{x}_i x_j)$ as feedforward to the ith mode, where x_j is the measurement result at the jth mode. Note that this measurement-based reversibility is specific to QND, controlled-NOT, and controlled π-phase-shift interactions.

We consider removing the jth mode from the cluster state through the erasing technique [Fig. 1(a)]. In this case, x quadrature of the jth mode is measured, and feedforward to any mode of $i \in N_j$ is performed. In the Heisenberg picture, the operators after the feedforward are $\hat{p}_i' = \hat{Z}_i^\dagger(-x_j)\hat{p}_i\hat{Z}(-x_j) = \hat{p}_i - x_j$ for each $i \in N_j$. As a resulting state, we obtain

$$\left\langle \Delta \left(\hat{p}_i' - \sum_{k \in N_{i|j}} \hat{x}_k \right)^2 \right\rangle < \frac{1}{2} \quad \text{for } i \in N_j,$$

$$\left\langle \Delta \left(\hat{p}_i - \sum_{k \in N_i} \hat{x}_k \right)^2 \right\rangle < \frac{1}{2} \quad \text{for } i \in G' - N_j,$$
(4)

where $G' = G|j$. Thus inequality (2) is preserved even after the removal operations. Therefore the jth mode is removed from the graph G, and cluster-type entanglement remains present among the resulting graph G'.

The same technique can be also used for removing modes while still preserving the connections or entanglement of their neighbors, so-called wire shortening [6]. Here we consider the modes 1, 2, 3, and 4 in a cluster state constituting a wire from 1 to 4, $N_2 = \{1,3\}$ and $N_3 = \{2,4\}$, while the first mode and the fourth mode are not neighbors, as shown in Fig. 1(b). The wire shortening requires that there are no other neighbor modes of either the second or third mode, but this requirement can be easily met by removing such modes prior to the wire shortening. With local phase shifts of $\{\pi, -\pi/2, \pi/2, 0\}$ on each $\{1,2,3,4\}$th mode, the wire becomes a ring [14]. Thus shortening of this wire corresponds to removing the second and third modes from the ring. In the case of the ring, this operation is done by measuring x quadratures of the second and third modes and performing feedforward to the fourth and first modes, $\hat{Z}_4(-x_2)$ and $\hat{Z}_1(-x_3)$. In the case of the wire, the operation is equivalent to measuring $\hat{p}_2$ and $\hat{p}_3$ and performing $\hat{Z}_4(-p_2)$ and $\hat{Z}_1(-p_3)$; as a resulting state, we obtain the cluster state with nullifiers $(\hat{p}_1 + \hat{x}_4 - \sum_{i \in N_{1|4}} \hat{x}_i)$

(a) Removing a mode from a cluster state.

(b) Wire-shortening.

(c) Realizing scheme of shaping a cluster state.
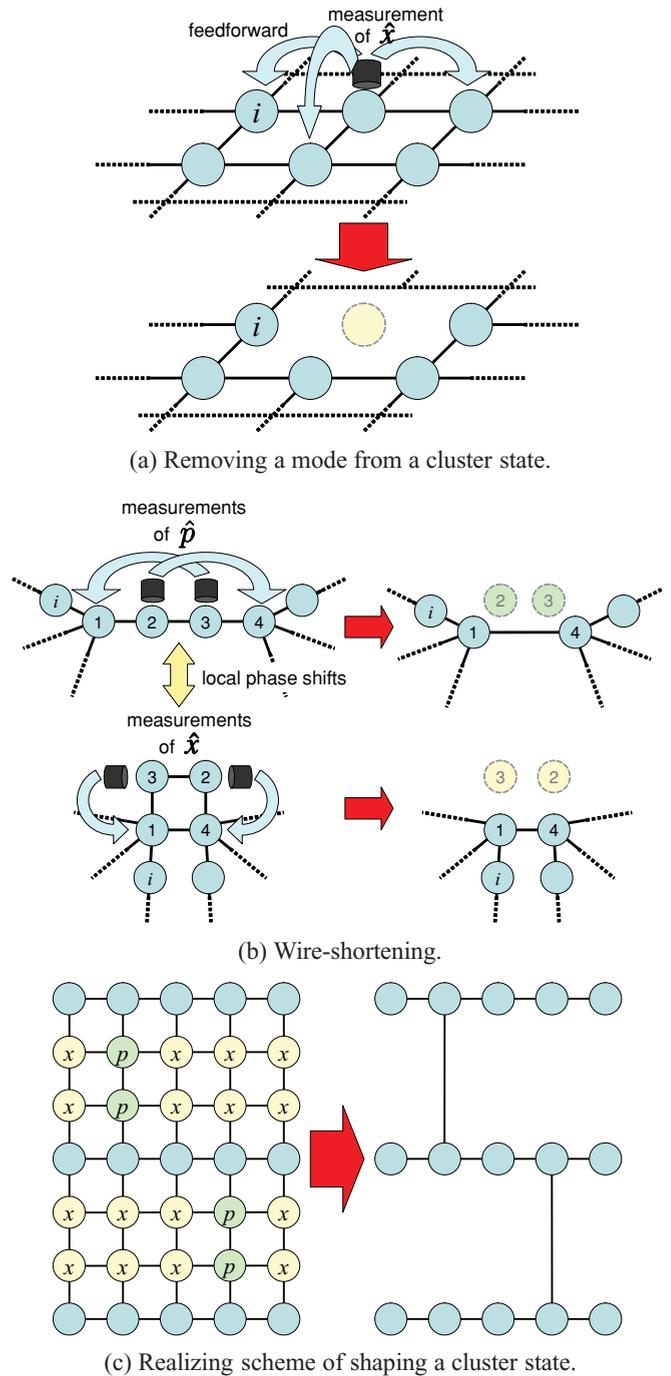
FIG. 1. (Color online) Cluster-state shaping using measurement and feedforward. Measuring x simply removes the modes, while measuring p removes the modes with their quantum correlation reconstructed in their neighbors.

and $(\hat{p}_4 + \hat{x}_1 - \sum_{j \in N_{4|1}} \hat{x}_j)$. Thus the first and fourth modes are directly connected in the resulting state. Note that the signs of $\hat{x}_1$ and $\hat{x}_4$ are opposite compared with Eq. (1) because of the local phase shifts from the wire to the ring. With these two transformations—removing unwanted modes and wire shortening—we can generate many desired cluster states from a sufficiently large two-dimensional lattice [6], as shown in Fig. 1(c).

(a) Removing an edge mode from a four-mode cluster state.

(b) Removing an inward mode from a four-mode cluster state.

(c) Wire-shortening from a four-mode cluster state.

(d) Experimental setup for removing an edge mode from a four-mode cluster state.
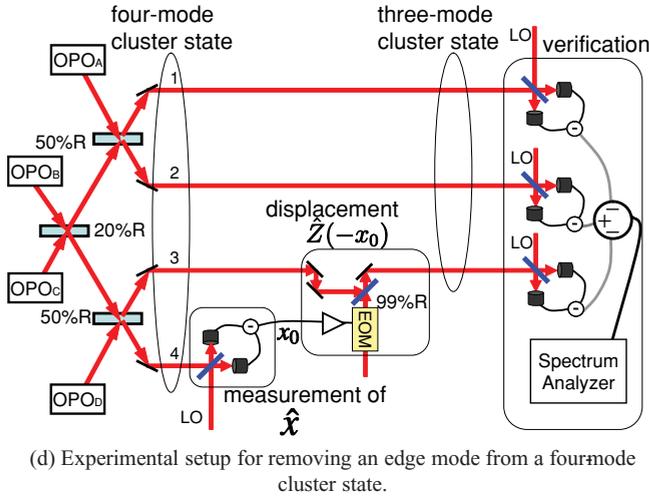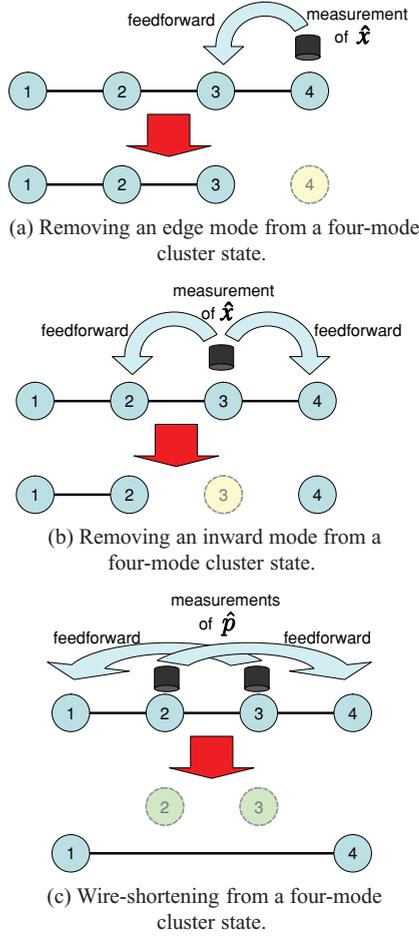
FIG. 2. (Color online) Schematic of cluster state shaping and our experimental implementation. OPO, subthreshold optical parametric oscillator generating a squeezed vacuum state; LO, optical local oscillator for homodyne detection.

We experimentally demonstrate the preceding shaping operations on a four-mode linear cluster state. Two of the following three experiments correspond to the removal of a mode, either at the edge of the cluster or within the cluster state [Figs. 2(a) and 2(b)]. The other experiment is wire shortening [Fig. 2(c)].

III. EXPERIMENTAL SETUP

Figure 2(d) is a schematic of our experimental implementation of Fig. 2(a). This setup consists of generating a four-mode cluster state, shaping via measurement and feedforward, and verification measurement. As a light source, we utilize a continuous-wave Ti:sapphire laser with a wavelength of 860 nm. Four squeezed-vacuum states are generated from four subthreshold optical parametric oscillators (OPOs). Each OPO is a bowtie-shaped cavity of 500 mm in length with a 10 mm long PPKTP crystal as a nonlinear medium [15], which is pumped by the second harmonic (430 nm in wavelength) of Ti:sapphire output. We generate a four-mode linear cluster state from four squeezed-vacuum states using three beam splitters with beam-splitting ratios 20:80, 50:50, and 50:50, respectively [9,14]. In this experiment, ± 1 MHz sidebands are quantum modes, while 98 kHz, 138 kHz, and 220 kHz modulations are used as phase references. Squeezing levels of resource squeeze vacuum states are about -5 dB. The quantum correlation of the initial cluster states satisfies inequality (2):

$$\left\langle \Delta\left(\hat{p}_i - \sum_{j \in N_j} \hat{x}_b\right)^2\right\rangle < 0.25 \pm 0.01 < \frac{1}{2}$$
$$\text{for } i \in 1,2,3,4; \qquad (5)$$

thus any mode of this cluster state is inseparable from the other modes.

In shaping operations, the modes being removed are measured via homodyne detection. In order to perform feedforward, the electric signal of the detection outcome is amplified and drives an electro-optical modulator traversed by an auxiliary beam with the power of 200 μW, which is subsequently coupled with the neighbor mode of the measured mode by an asymmetric beam splitter (99:1).

Modes to be measured and to be suffered from feedforward depend on the shaping [Figs. 2(a)–2(c)]. For verification, remaining modes are measured via other homodyne detections. The measurement-outcome electric signals are combined and then sent to a spectrum analyzer in order to check the correlations between output quadratures. The powers of the optical local oscillators (LOs) are about 5 mW. The detector's quantum efficiencies are greater than 99%, and the interference visibilities to the LOs are, on average, 96%.

IV. EXPERIMENTAL RESULTS

First, we demonstrate removal of the edge fourth mode from a four-mode linear cluster state, as shown in Fig. 2(a). Here we measure x quadrature of the fourth mode and perform feedforward to the third mode, $\hat{Z}_3(-x_4)$, and we verify entanglement among the remaining modes. Figures 3(a)–3(c) show experimental results of variances of nullifiers (red traces) suppressed below the cluster criteria inequality (2) (blue lines):

$$\langle\Delta(\hat{p}_1 - \hat{x}_2)^2\rangle = 0.14 \pm 0.01 < \tfrac{1}{2},$$
$$\langle\Delta(\hat{p}_2 - \hat{x}_1 - \hat{x}_3)^2\rangle = 0.22 \pm 0.01 < \tfrac{1}{2}, \qquad (6)$$
$$\langle\Delta(\hat{p}_3 - \hat{x}_2)^2\rangle = 0.26 \pm 0.01 < \tfrac{1}{2}.$$

(a) $\langle(\hat{p}_1 - \hat{x}_2)^2\rangle$.

(b) $\langle(\hat{p}_2 - \hat{x}_1 - \hat{x}_3)^2\rangle$.

(c) $\langle(\hat{p}_3 - \hat{x}_2)^2\rangle$.

(d) $\langle(\hat{p}_1 - \hat{x}_2)^2\rangle$.

(e) $\langle(\hat{p}_2 - \hat{x}_1)^2\rangle$.

(f) Resulting state of the fourth mode.

(g) $\langle(\hat{p}_1 + \hat{x}_4)^2\rangle$.

(h) $\langle(\hat{p}_4 + \hat{x}_1)^2\rangle$.
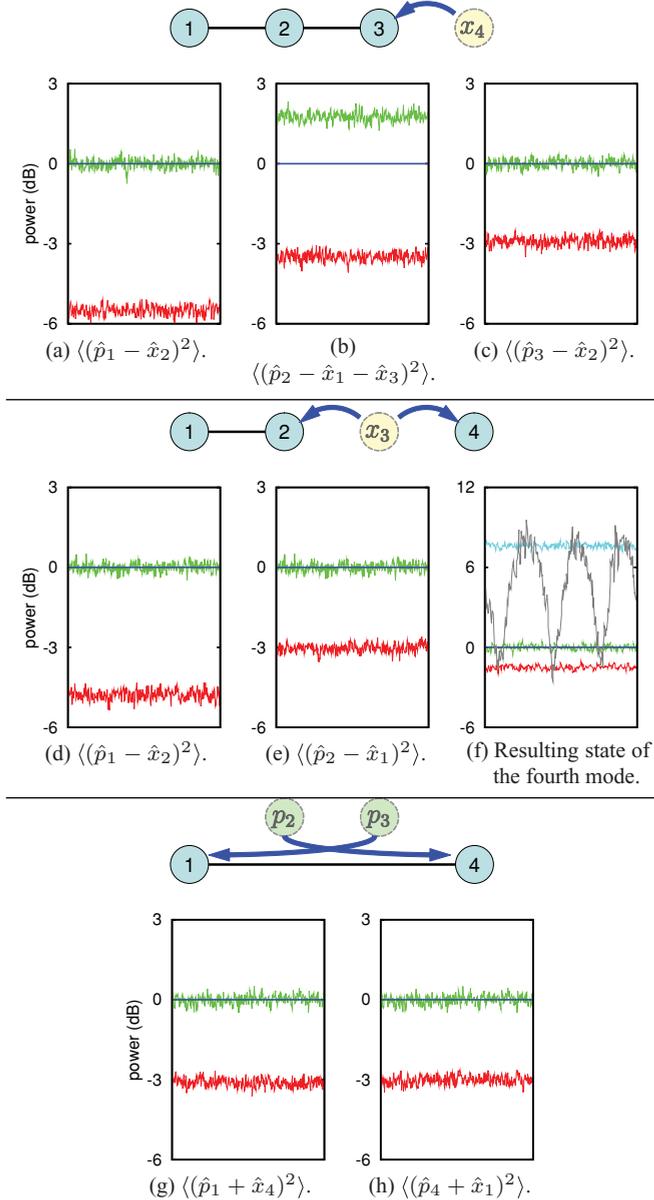
FIG. 3. (Color) Experimental results. (a)–(c) Quantum correlations of remains of three modes in experiment represented in Fig. 2(a). Experimental results (red traces) are compared with vacua states (green traces), relative to two SNLs (=1/2, blue lines). (d), (e) Remaining quantum correlations between the first and second modes in the experiment of Fig. 2(b). (f) Resulting state of the fourth mode. Variance of the squeezed quadrature (red trace), antisqueezed quadrature (cyan), and observed variance with LO phase scanned (gray) are compared with vacuum state (green). (g), (h) Reconstructed quantum correlations in the wire-shortening experiment represented in Fig. 2(c).

Therefore we successfully remove the fourth mode with preserving entanglement among the remaining modes.

Next, we also remove the inward third mode from the four-mode cluster state, as shown in Fig. 2(b). This time, we measure x quadrature of the third mode and perform feedforward to the second and fourth modes, $\hat{Z}_2(-x_3)$ and $\hat{Z}_4(-x_3)$. Theoretically, the resulting states become a two-mode cluster state (the first and second modes) and a squeezed

state (the fourth mode). As Figs. 3(d) and 3(e) show, we observed quantum correlations between the first and second modes:

$$\langle\Delta(\hat{p}_1 - \hat{x}_2)^2\rangle = 0.17 \pm 0.01 < \tfrac{1}{2},$$
$$\langle\Delta(\hat{p}_2 - \hat{x}_1)^2\rangle = 0.25 \pm 0.01 < \tfrac{1}{2}. \qquad (7)$$

Since they satisfy inequality (2), these modes are entangled. Meanwhile, the fourth mode recovers its squeezed property, as shown in Fig. 3(f). Variance of squeezed quadrature is -1.5 ± 0.2 dB relative to the SNL. Thus a two-mode cluster state and a squeezed vacuum are obtained from a four-mode cluster state.

Finally, we perform wire shortening, as shown in Fig. 2(c). Again, we start with the four-mode cluster state, and then we measure p quadratures of the second and third modes and perform feedforward to the fourth and first modes, $\hat{Z}_4(-p_2)$ and $\hat{Z}_1(-p_3)$. Figures 3(g) and 3(h) show quantum correlations of the resulting state. The reconstructed quantum correlations are

$$\langle\Delta(\hat{p}_1 + \hat{x}_4)^2\rangle = 0.25 \pm 0.01 < \tfrac{1}{2},$$
$$\langle\Delta(\hat{p}_4 + \hat{x}_1)^2\rangle = 0.24 \pm 0.01 < \tfrac{1}{2}, \qquad (8)$$

satisfying inequality (2). Therefore two modes are removed, while their quantum correlations are preserved between their neighbors.

Observable quantum correlations in Figs. 3(c), 3(e), 3(g), and 3(h) are degraded by about 2 dB from the original resource squeezing levels of -5 dB. The degradation corresponds to a cost of the top-to-bottom approach because generating a large cluster state requires extra QND interactions which are imperfect due to finite-squeezed resources [16]. Nonetheless, technological progress toward increasing the experimental squeezing levels [17,18] will improve the cluster state shaping.

In conclusion, we have demonstrated experimentally how to remove an arbitrary node from a continuous-variable cluster state and how to shorten any quantum wires of such a state, where both transformations are performed in unconditional fashion via quantum erasure. In our experiment, all variations of this cluster shaping have been demonstrated on a four-mode linear cluster state. These two transformations can provide flexibility of fixed large-scale cluster states and transform them into appropriate forms for desired quantum operations.

[1] R. Raussendorf, D. E. Browne, and H. J. Briegel, Phys. Rev. A **68**, 022312 (2003).

[2] N. C. Menicucci, P. van Loock, M. Gu, C. Weedbrook, T. C. Ralph, and M. A. Nielsen, Phys. Rev. Lett. **97**, 110501 (2006).

[3] N. C. Menicucci, S. T. Flammia, and O. Pfister, Phys. Rev. Lett. **101**, 130501 (2008).

[4] R. Filip, Phys. Rev. A **67**, 042111 (2003).

[5] Y. Miwa, R. Ukai, J. Yoshikawa, R. Filip, P. van Loock, and A. Furusawa, in *Technical Digest of CLEO/QELS2010, JThE26* (Optical Society of America, San Jose, 2010); Y. Miwa, J. Yoshikawa, R. Ukai, R. Filip, and A. Furusawa, e-print arXiv:1007.0314v2 [quant-ph].

[6] M. Gu, C. Weedbrook, N. C. Menicucci, T. C. Ralph, and P. van Loock, Phys. Rev. A **79**, 062318 (2009).

[7] M. Varnava, D. E. Browne, and T. Rudolph, Phys. Rev. Lett. **97**, 120501 (2006).

[8] P. Walther, K. J. Resch, T. Rudolph, E. Schenck, H. Weinfurter, V. Vedral, M. Aspelmeyer, and A. Zeilinger, Nature (London) **434**, 169 (2005).

[9] P. van Loock, C. Weedbrook, and M. Gu, Phys. Rev. A **76**, 032321 (2007).

[10] M. Ohliger, K. Kieling, and J. Eisert, e-print arXiv:1004.0081v2 [quant-ph].

[11] J. Zhang and S. L. Braunstein, Phys. Rev. A **73**, 032318 (2006).

[12] V. B. Braginsky and F. Y. Khalili, *Quantum Measurement* (Cambridge University Press, Cambridge, 1992).

[13] P. van Loock and A. Furusawa, Phys. Rev. A **67**, 052315 (2003).

[14] M. Yukawa, R. Ukai, P. van Loock, and A. Furusawa, Phys. Rev. A **78**, 012301 (2008).

[15] S. Suzuki, H. Yonezawa, F. Kannari, M. Sasaki, and A. Furusawa, Appl. Phys. Lett. **89**, 061116 (2006).

[16] J. Yoshikawa, Y. Miwa, A. Huck, U. L. Andersen, P. van Loock, and A. Furusawa, Phys. Rev. Lett. **101**, 250501 (2008).

[17] Y. Takeno, M. Yukawa, H. Yonezawa, and A. Furusawa, Opt. Express **15**, 4321 (2007).

[18] H. Vahlbruch, M. Mehmet, S. Chelkowski, B. Hage, A. Franzen, N. Lastzka, S. Gossler, K. Danzmann, and R. Schnabel, Phys. Rev. Lett. **100**, 033602 (2008).